

COMPARATIVE STUDY ON TWO ANALYTICAL MECHANICAL-BASED METHODS FOR DERIVING FRAGILITY CURVES TARGETED TO MASONRY SCHOOL BUILDINGS

Cattari S.¹, Alfano S.¹, Ottonelli D.¹, Saler E.^{2,3} and da Porto F.²

¹ Dept. of Civil, Chemical and Environmental Engineering, University of Genoa
Via Montallegro 1, 16145 Genoa
e-mail: {serena.cattari,sara.alfano,daria.ottonelli}@unige.it

² Dept. of Geosciences, University of Padova
Via Gradenigo 6, 3513 Padova
{elisa.saler, francesca.daporto}@unipd.it

³ Dept. of Civil, Environmental and Mechanical Engineering, University of Trento
Via Mesiano 77, 38123 Trento

Abstract

Seismic events across several countries in the world have highlighted that strategic buildings, such as schools, may exhibit vulnerability levels that are in some cases higher than those of ordinary buildings. It follows the urgent need of reliable risk analyses to support the decision-making for large-scale mitigation policies. To this aim, the derivation of fragility curves, able to capture typological and constructive characteristics, constitutes an essential requisite. Within this context, the paper presents a comparative study on the use of two analytical-mechanical based methods for assessing fragility curves of Italian masonry school buildings. These are very often characterized by a number of stories rarely higher than three, presence of rigid floors, significant inter-story height, and great distance between transverse walls. Among the others, analytical approaches, either based on numerical or mechanical models, are more suitable to capture the effects of such features on the seismic vulnerability. The two methods discussed in the paper are “Vulnus Vb 4.0-2009”, developed at the University of Padova and based on the integrated use of mechanical and macroseismic approaches, and “DBV-Masonry (Displacement Based Vulnerability)”, a pure mechanical-based model developed at the University of Genoa. Both methods are applied to a stock of 14 masonry schools, selected as prototypes of Italian school masonry buildings. The critical review and comparative application of the two methods allow highlighting their similarities and differences in assessing the fragility associated to in-plane and out-of-plane failure mechanisms. Moreover, as some of the selected schools had been hit by the 2016-17 Central Italy earthquake sequence, the evidence of the real response allows assessing the actual reliability of the methods.

Keywords: Masonry school building· Fragility curves· Analytical-mechanical models· Seismic vulnerability.

1 INTRODUCTION

Schools constitute a key stone for the social and cultural life of people, beside to represent an essential place for supporting the growing of new generations. Despite the role they play, reconnaissance surveys of damage after many seismic events (*e.g.* as documented in Italy [1], [2]) have highlighted how strategic buildings or high-exposure buildings, such as schools, can present high levels of vulnerability and inadequate performance, in some cases comparable to those of ordinary ones. This has been confirmed also by vulnerability studies carried out in various countries across the world (*e.g.*, for Nepal [3], and for Iran [4]). The attention to the topic is also testified by various recent studies addressed to reduce risk and enhance resilience of schools (*e.g.*, [5],[6]), as well as some worldwide programs aimed to promote “safer schools” (*e.g.*, [7],[8]).

As known, derivation of fragility curves, able to capture the typological and constructive characteristics of the examined building stock, is a key point for reliable risk analyses, in order to support decision-making for large-scale mitigation policies. To date, few studies available in the literature have focused on fragility of unreinforced masonry (URM) schools. Fragility curves based on empirical approaches constitute a valuable resource, being based on the direct observation of damage (*e.g.*, derived for Peruvian [9] and Nepalese [10] schools). However, being usually based on a limited stock, their derivation faces the critical issues of less robust data, from a statistical point of view, than ordinary buildings. As a consequence, analytical approaches, either based on numerical or mechanical models [*e.g.*, [6], [11], [12], [13], [14]], are more suitable to capture the effects of specific features that affect the seismic vulnerability of such buildings.

Focusing on URM schools in Italy, the inventory of the Italian Ministry of Education, dated to 2005, indicates about 50,000 schools on the Italian territory, of which about 21% are masonry buildings. With respect the total URM stock, the distribution across the age is: 20% Pre1920, 18% 1921-45, 24% 1946-60, 20% 1961-75, 8% Post76; moreover, for the 10% the age is not available (indicated as NA in Figure 1). These schools are very often characterized:

- by low-rise, *i.e.*, the number of stories is rarely higher than three (see Figure 1);
- irregular plan: plans characterized by “T”, “L”, “C” shapes or with internal court. The latter is more frequently found for buildings that date back before 1920, in case their use changed along time;
- significant inter-story height;
- great distance between transverse walls;
- presence of rigid floors.

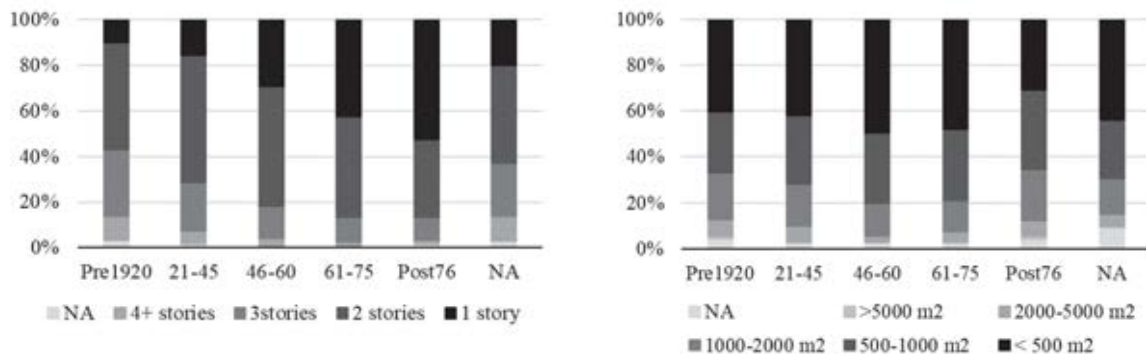


Figure 1. Distributions of Italian schools present in the Italian Ministry of Education inventory dated to 2005.

Within this context and being aware of the aforementioned high relevance of risk and resilience assessments of the national school asset, the Italian Civil Protection Department (DPC) conveyed the effort of several Italian Universities to update the National Risk Assessment already released in 2018 ([15], [16]), in order to include not only residential buildings but also other strategic classes, such as schools and churches. Thus, within the 2019–2021 research agreement between the Civil Protection Department (DPC) and the Network of University Laboratories for Earthquake Engineering (ReLUIS), the work package WP4 “Seismic Risk Maps -MARS” has been specifically conceived to address this scope [17]. One of the aims of the project is the derivation of seismic fragility models, able to describe the vulnerability of classes of schools characterized by seismic homogenous behavior.

Within this framework, the paper presents a comparative study on the use of two analytical-mechanical based methods for assessing fragility curves of schools; both of them have been adopted in the MARS project.

The two methods discussed in the paper are “Vulnus Vb 4.0-2009”, a hybrid model developed at the University of Padova, based on the integrated use of mechanical and macroseismic approaches [18], and the “DBV-*Masonry* (Displacement Based Vulnerability)”, a pure mechanical-based model originally developed at the University of Genoa [19] and further developed within the MARS project. Both methods assume a lognormal cumulative distribution to define fragility curves, that is thus defined by two parameters: the median value (i.e., the intensity measure, in this case the Peak Ground Acceleration, associated to the 50% probability of attaining the damage level under examination, indicated as IM_{DLi}); and the log-normal standard deviation (β_{DLi}). The fragility curves are associated to five damage levels (DL_i , $i = 1 \dots 5$), aimed to be consistent with those proposed in the EMS98 scale [20].

In this study, both methods were applied to a stock of 14 masonry schools, selected as prototypes of Italian school masonry buildings and described in §2. The assumptions on which the two methods are based are briefly recalled in §3, while the main aim of this contribution, which is the critical review and comparative application of the two methods, is presented in §4 by adopting – when possible – analogous hypotheses to estimate the seismic fragility of the schools under examination. Moreover, as some of the selected schools had been hit by the 2016-17 Central Italy earthquake sequence, the evidence of the real response allows some considerations on the reliability of the methods to be provided (§5).

2 DESCRIPTION OF THE ANALYZED PROTOTYPE SCHOOLS

The stock analyzed in the following is composed of 14 school buildings selected from three regional databases provided by the University of Naples and Genoa (database A) [21], the University of Padua (database B) [22] and the University of Trieste (C) [23]. Database A [21] includes school buildings from various areas of Central Italy; it groups data collected during support activity made by the ReLUIS consortium and DPC [24], requested by the Reconstruction Commissioner, nominated after the 2016/2017 Central Italy earthquake. Instead, database B and C refer to the data collected in the municipal area of Padua (B) and in the regional area of Friuli-Venezia Giulia (C). Database A, B and C contain 54, 25 and 92 masonry schools, respectively.

The 14 school buildings extracted from these databases were identified to be representative of Italian masonry schools. They were used within the MARS project – Task 4.7 [17] to derive fragility curves representative of sub-types with homogeneous seismic behavior, adopting them as “prototype buildings”.

The taxonomy for identifying these sub-types is based on the data available in the inventory set by the Italian Ministry of Education dated to 2005, namely: structural material (e.g.,

reinforced concrete, masonry, steel) and seismic resistant system (e.g., frame, shear walls); number of stories (i.e., 1,2,3, >4); plan area (i.e., <500 m², 500-1000 m², 1000-2000 m², 2000-5000 m², and >5000m²); diaphragm type (e.g., concrete slab with clay units, wooden floor); and roof type (i.e., flat, inclined, or mixed). Starting from this inventory, specific sub-types were defined to cover most of the Italian school building asset. In fact, as shown in Figure 1, the Italian URM school stock is mostly represented by low structures (mainly 2-story), with limited floor area (in most cases < 1000 m²), and mainly built before 1975.

These criteria addressed the choice of the 14 prototype schools. Table 1 gives an overview of the analyzed set in terms of construction age, plan shape, plan gross area, and inter-story height; nine schools date back to 1945, while the 65% of the stock is characterized by two floors, to better represent the national asset. Each school is identified by an alphanumeric ID, while the database from which the school was extracted is indicated in brackets.

While other literature works are dedicated to derive fragility curves representative the overall URM school taxonomy [25], as already specified in §1, this paper focuses on their derivation by explicitly referring to the original features of each prototype school (referred as the “as it is state” in the following): this is to facilitate a more accurate comparison between the two methods adopted in the paper and briefly recalled in §3.

ID School	Age	N. floors	Inter-story height [m]	Plan configuration	Plan gross area [m ²]
S1 (A)	Before 1919	3	NA	Elongated rectangular	< 500
S2 (B)	Before 1919	2	5.8 – 5.4	U-shape	> 2000
S3 (A)	Before 1919	2	NA	Cloister	1000-2000
S4 (A)	Before 1919	3	NA	C-shape	1000-2000
S5 (A)	1921-1945	2	4.4	Elongated rectangular	500-1000
S6 (A)	1921-1945	2	4.5 – 3.5	Rectangular	< 500
S7 (C)	1921-1945	2	4.6	Rectangular	< 500
S8 (C)	1921-1945	2/3	4.1 – 4.1 – 7.3/6.5	C-shape	1000-2000
S9 (A)	1921-1945	2	4.3 – 4.5	T-shape	500-1000
S10 (B)	1946-1960	2	3.15	L-shape	1000-2000
S11 (A)	1946-1960	2	3.0 – 2.9	Rectangular	< 500
S12 (C)	1946-1960	2	3.8	Rectangular	< 500
S13 (A)	1961-1975	1	3.5	Squared	< 500
S14 (A)	After 1976	1	3.0	Squared	< 500

Table 1. General data of examined prototype school buildings (NA stands for Not Available).

Figure 2 shows, for some prototype schools, a view of the plan, together with photos aimed to provide a general overview of the building. The variety of plans confirms what already introduced in §1 about the recurrence of irregular shapes.



Figure 2. Plan shape and photos of some analyzed prototype schools.

For each prototype school, the basic data required for their typological and constructive characterization, as well as for the application of the two examined methods were collected, such as: the masonry type; the type of intermediate floors and roof; the resistant area for each story (in both directions); and the systemic presence of structural details, such as the presence of reinforced concrete (r.c.) ring beams or steel tie rods. Masonry type resulted quite heterogeneous. Conversely, intermediate floors was mainly ascribable to concrete slab with hollow clay blocks.

ID School	Resistant area [%]		Masonry type	Floor diaphragms	Roof	Structural Details
	X	Y				
S1	2.9	9.7	Solid bricks and lime mortar	Wooden floor	Wooden roof	Neither ring beams nor tie-rods systematic
S2	5.7 5.1	4.3 4.1	Solid bricks and lime mortar	r.c. slab	Wooden roof	r.c. ring beams
S3	9.7	8.0	Rubble stone	Vaults / Vaults with steel beams / r.c. slab with hollow clay blocks	Wooden roof	Partial presence of tie rods
S4	8.9 8.8 8.3	6.6 5.5 5.5	Solid bricks and lime mortar	Vaults	Wooden roof	Neither ring beams nor tie-rods systematic
S5	12.0 7.4	11.0 5.9	Rubble stone	Vaults with steel beams / r.c. slab with hollow clay blocks	Concrete slab with hollow clay blocks	r.c. ring beams along the perimeter of the roof
S6	6.9 7.6	4.2 4.3	Solid bricks and lime mortar	Concrete slab with hollow clay blocks	Concrete slab with hollow clay blocks	Neither ring beams nor tie-rods systematic
S7	5.9 5.9	4.8 4.6	Rubble stone with courses made by solid bricks	Concrete slab with hollow clay blocks / wooden floor / r.c. slab	Concrete slab with hollow clay blocks	r.c. ring beams
S8	5.4 5.0 6.8	6.9 5.6 8.7	Stone ashlar well-arranged	Concrete slab with hollow clay blocks / wooden floor	Wooden roof	r.c. ring beams on the first floor
S9	10.2 9.1	7.7 6.6	Stone ashlar well-arranged	Concrete slab with hollow clay blocks	Concrete slab with hollow clay blocks	r.c. ring beams along the perimeter of the roof
S10	2.7	1.9	Solid bricks and lime mortar	Concrete slab with hollow clay blocks	Concrete slab with hollow clay blocks	r.c. ring beams
S11	9.4 9.8	8.8 9.4	Simple stone with courses made by solid bricks	Concrete slab with hollow clay blocks	Concrete slab with hollow clay blocks	r.c. ring beams
S12	7.0	4.1	Solid bricks and lime mortar	Concrete slab with hollow clay blocks	Concrete slab with hollow clay blocks	r.c. ring beams
S13	3.7	3.7	Hollow blocks with cement mortar	Concrete slab with hollow clay blocks	Concrete slab with hollow clay blocks	r.c. ring beams
S14	Na	Na	Regular masonry	Rigid floor	Rigid floor	Neither ring beams nor tie-rods systematic

Table 2. Typological and constructive features of analyzed prototype schools.

2.1 Mechanical parameters adopted for prototype schools

For the application of the methods referred to in §3, the range of variation of the mechanical parameters of the masonry must be defined, in particular: the shear strength (τ_0), the masonry compressive strength (f_c), and the tangential modulus of elasticity (G). Since for most cases, direct mechanical characterization data were not available, reference values (plausible for the masonry types under examination) were assumed according to literature data ([26], [27], [28],

[29], [30], [31]). More specifically, the intervals recommended in the Italian Technical Code [32] were taken as reference. In particular, this Code provides firstly a basic range of values representative for a masonry that doesn't strictly follow the rules of thumbs (Table C8.5.I in [32]). Then corrective coefficients, which in most cases lead to an increase to the basic values, are proposed too (Table C8.5.II in [32]) with the aim of accounting for specific features which may influence the response of the masonry ([27], [33]), such as good quality mortar; good transversal connection between leaves; the presence of courses aimed to improve the horizontality of layers. The list of such corrective coefficients is summarized in Table 3 for sake of completeness.

Correction coefficient for the state of the art	Masonry Types							
	A	B	C	D	E	F	G	H
Good quality mortar	1.5	1.4	1.3	1.5	1.6	1.2	(^b)	1.2
Courses or borders ^a	1.3	1.2	1.1	1.2	-	-	-	-
Transverse connections ^a	1.5	1.5	1.3	1.3	1.2	1.2	1.3 (^b)	-

^a Correction coefficient relate solely to strength parameters

^b "Good mortar" corresponds to a mortar with an average compressive strength (f_{mj}) greater than 2 MPa. In this case the corrective coefficient can be set equal to $f_{mj}^{0.35}$ (f_{mj} in Mpa).

Legend of masonry types: A – Random rubble stone masonry (pebbles, erratic, irregular stone); B – Uncut stone masonry with facing walls of irregular thickness; C – Ashlar masonry with good bonding; D – Irregular soft stone masonry (tuff, limestone, etc.); E – Regular soft stone masonry (tuff, limestone, etc.); F – Dressed rectangular stone masonry with no-soft stone; G – Solid bricks with lime mortar; H – Hollow blocks with cement mortar

Table 3. Correction coefficient for different types of masonry as proposed in [32].

Following this approach, for each school, the most plausible ranges of mechanical parameters were adopted. Smaller intervals of variation correspond to higher level of knowledge (see for example S9 and S5 in Figure 3). Conversely, in case of scarce data, the lack of knowledge lead to a higher residual uncertainty (i.e., a larger range of variation of the parameters). In particular, the highest range of variation was defined as follows (see for example S6 in Figure 3): the minimum value corresponds to the minimum proposed in Italian Technical Code [32]; the maximum value corresponds to the maximum proposed in the code, to which all the possible corrective coefficients were applied. The mechanical parameters of each school building used for the application of the analytical-mechanical models are reported in Table 4.

ID School	Specific feature of the masonry types of the school	fc [MPa]	τ_0 [MPa] (min- max)		G [MPa] (min-max)	
		MEAN	MIN	MAX	MIN	MAX
S1	Low quality of mortar joints and stone texture	2.4	0.035	0.091	320	480
S2	NA	2.6	0.05	0.253	400	900
S3	NA	2.0	0.032	0.126	344	858
S4	Good mortar	2.6	0.075	0.253	600	900
S5	Low quality of mortar joints and stone texture	2.0	0.0245	0.0357	272	384
S6	NA	2.4	0.05	0.253	400	900
S7	Brick courses	2.4	0.043	0.072	346	492
S8	NA	2.7	0.056	0.074	500	660
S9	Good mortar and good transversal connection	3.4	0.0945	0.125	650	858
S10	NA	2.7	0.05	0.253	400	900
S11	Brick courses	2.9	0.062	0.106	500	858
S12	Good mortar	4.8	0.075	0.195	600	900
S13	NA	6.0	0.08	0.204	875	1680
S14	NA	2.6	0.05	0.253	400	900

Table 4. Mechanical parameters adopted for each school building (NA stands for Not Available).

Young's modulus was conventionally assumed to be three times the shear modulus (G). Due to the limited influence of the masonry compressive strength in case of low-moderate axial load acting on walls (as usually the case of existing buildings), it was assumed deterministic and equal to the mean value of the range proposed in Italian Code [32] .







Panel	Transversal section	Mechanical parameters																					
		S9 - Well-arranged stone masonry <table> <tr> <th>Good mortar</th><th>Brick courses</th><th>Transverse connection</th></tr> <tr> <td>Yes</td><td>No</td><td>Yes</td></tr> <tr> <td>1.3</td><td>1.1</td><td>1.3</td></tr> <tr> <td colspan="2">MIN</td><td>MAX</td></tr> <tr> <td>τ_0 [MPa]</td><td>0.0946</td><td>0.125</td></tr> <tr> <td>f_c [MPa]</td><td colspan="2">3.4</td></tr> <tr> <td>G [MPa]</td><td>650</td><td>858</td></tr> </table>	Good mortar	Brick courses	Transverse connection	Yes	No	Yes	1.3	1.1	1.3	MIN		MAX	τ_0 [MPa]	0.0946	0.125	f_c [MPa]	3.4		G [MPa]	650	858
Good mortar	Brick courses	Transverse connection																					
Yes	No	Yes																					
1.3	1.1	1.3																					
MIN		MAX																					
τ_0 [MPa]	0.0946	0.125																					
f_c [MPa]	3.4																						
G [MPa]	650	858																					
		S5 - Rough cut stone <table> <tr> <th>Good mortar</th><th>Brick courses</th><th>Transverse connection</th></tr> <tr> <td>No</td><td>No</td><td>No</td></tr> <tr> <td colspan="2">MIN</td><td>MAX</td></tr> <tr> <td>τ_0 [MPa]</td><td>0.0245</td><td>0.036</td></tr> <tr> <td>f_c [MPa]</td><td colspan="2">2.0</td></tr> <tr> <td>G [MPa]</td><td>272</td><td>384</td></tr> </table> <p>These mechanical parameters were reduced due to the poor masonry quality observed (as indicated by Code [32])</p>	Good mortar	Brick courses	Transverse connection	No	No	No	MIN		MAX	τ_0 [MPa]	0.0245	0.036	f_c [MPa]	2.0		G [MPa]	272	384			
Good mortar	Brick courses	Transverse connection																					
No	No	No																					
MIN		MAX																					
τ_0 [MPa]	0.0245	0.036																					
f_c [MPa]	2.0																						
G [MPa]	272	384																					
	 <p>? UNKNOWN DATA</p>	S6 – Solid bricks and lime mortar <table> <tr> <th>Good mortar</th><th>Brick courses</th><th>Transverse connection</th></tr> <tr> <td>?</td><td>No</td><td>?</td></tr> <tr> <td>1.5</td><td>1.0</td><td>1.3</td></tr> <tr> <td colspan="2">MIN</td><td>MAX</td></tr> <tr> <td>τ_0 [MPa]</td><td>0.05</td><td>0.253</td></tr> <tr> <td>f_c [MPa]</td><td colspan="2">2.4</td></tr> <tr> <td>G [MPa]</td><td>400</td><td>900</td></tr> </table>	Good mortar	Brick courses	Transverse connection	?	No	?	1.5	1.0	1.3	MIN		MAX	τ_0 [MPa]	0.05	0.253	f_c [MPa]	2.4		G [MPa]	400	900
Good mortar	Brick courses	Transverse connection																					
?	No	?																					
1.5	1.0	1.3																					
MIN		MAX																					
τ_0 [MPa]	0.05	0.253																					
f_c [MPa]	2.4																						
G [MPa]	400	900																					

Figure 3. Frontal view and transversal section of masonry types of some prototype schools and final range of variation adopted for mechanical parameters.

3 BRIEF MENTION OF ANALYTICAL-MECHANICAL METHODS USED

3.1 Mechanics-based modelling procedure *Vulnus*

The first simplified modelling procedure applied to the selected prototype schools was the mechanics-based approach developed at the University of Padova, which has been already

effectively applied to different territorial areas (i.e., from an urban area [34] to a national scale [18]). The approach is based on the simplified mechanical modelling procedure *Vulnus 4.0* [35] [36], which allows fragility assessment of unreinforced masonry buildings (URM) to be carried out considering both in-plane (IP) and out-of-plane (OOP) mechanisms, together with an index of the structural quality from 2nd level GNDT form [37]. The analysis of a URM building provides three indexes:

- i_1 , expressing the ratio between the IP shear resistance and the weight of the building for the weakest plan direction;
- i_2 , expressing the susceptibility to OOP mechanisms (both overturning and flexural failures), through the implementation of linear kinematic analyses;
- i_3 , quantifying vulnerability factors which affect the structural behavior (e.g., irregularity in elevation).

Then, the indexes are combined through fuzzy set theory, obtaining three fragility curves (derived as log-normal cumulative probability functions): one expressing the most probable distribution, called *white*, a lower- and an upper-bound. The fragility analysis of prototype schools was carried out referring to *white* curves. The resulting fragility refers to a medium-severe damage level (DL2-3), intermediate DS between 2 (given by trigger of OOP mechanisms) and 3 (given by IP global shear failure), according to the European macro-seismic scale (EMS98) [20].

Each DL2-3 curve was then extended to five fragility curves, from DL1 (slight damage) to DL5 (complete collapse), through the calibration of a fragility model proposed in [19], based on a previously presented macro-seismic model from the literature [38].

Figure 4 synthetically summarizes the basics of the procedure. For further details on the procedure, please refer to [1].

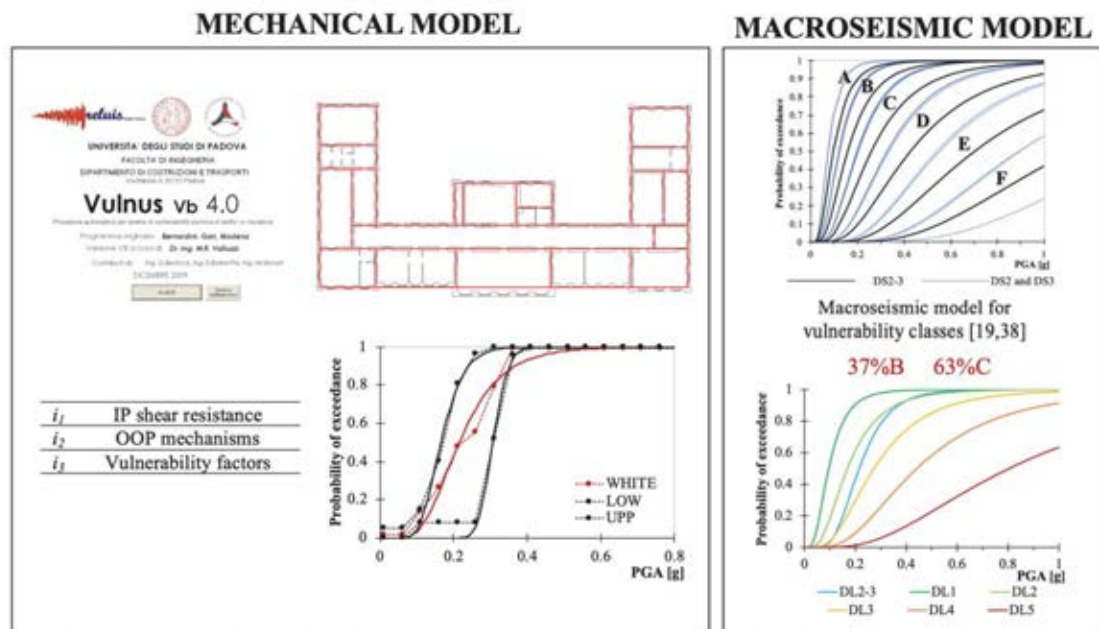


Figure 4. Basics of the *Vulnus* procedure.

3.2 DBV– *Masonry* model

The second simplified modelling procedure applied to the selected prototype schools was the mechanics-based approach developed at the University of Genoa [19].

The original approach was developed to derive fragility functions exclusively referring the global behavior of URM buildings associated to the in-plane walls response. The model firstly defines the capacity curve representative of the structural seismic response based on three variables (as in Figure 5): 1) the pseudo-elastic period of the structure T_y ; 2) the spectral acceleration at yielding A_y (equal to the ultimate one A_u , as no hardening is assumed); 3) the displacement capacity (associated to DL3 and DL4). The evaluation of these variables requires the definition of a limited number of mechanical and geometrical parameters, together with the assumption of a fundamental modal shape and the attribution of specific corrective factors (K_i), aimed to account for the effects induced by the large set of constructive and morphological details that usually characterize existing buildings. The analytical formulation basically makes reference to the Strong-Spandrels Weak-Piers (SSWP) behavior, thus under the simplified assumption, for the evaluation of the overall base shear, that all masonry piers fail at the same time. Then, some of the aforementioned factors (K_i) aims to correct this estimate in order to account for other possible behavior (like the Weak-Spandrels Strong-Piers – WSSP – or intermediate) induced by the lack of tie-rods and r.c. ring beams, or by the poor quality of spandrel elements (see [19] for further details). Once computed the capacity curve, the nonlinear static procedure based on the use of over-damped spectra [39] is adopted to compute the value of the IM that produces the attainment of DLs (IM_{DL}). To this aim, proper rules are introduced to define the intermediate DLs on the capacity curve (i.e., DL1 and DL2) and the corresponding equivalent damping values (ξ_{DL}) are evaluated. Finally, for the uncertainty propagation, various contributions are considered [19] and in particular the uncertainty associated to the structural capacity is computed by using the response surface method [40]. Figure 5 illustrates the basics of the method.

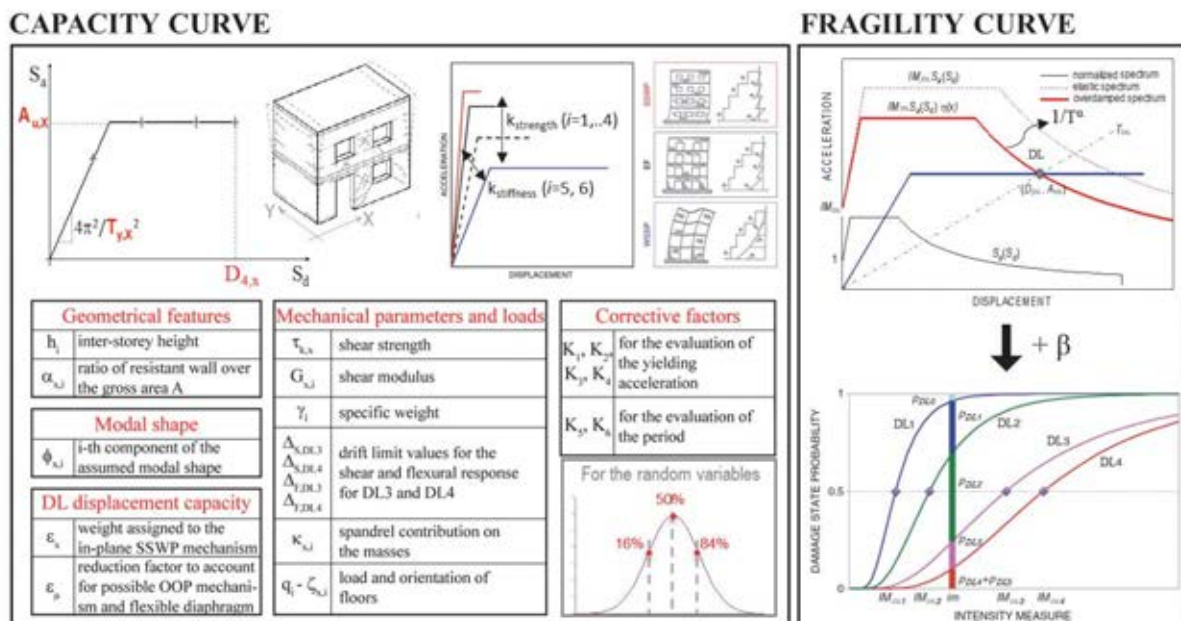


Figure 5. Basics of DBV-masonry model.

Starting from the original proposal of the model [19], within the MARS project as briefly summarized in the following, the authors from the University of Genoa made further refinements of the method that mainly concern, on the one hand, the estimate of the DLs displacement capacity, and, on the other hand, the evaluation of IM_{DL} .

As for the first issue, specific coefficients (ε_{μ}) aimed to limit the displacement capacity to introduce, even if in a simplified way, the possible activation of out-of-plane (OOP) mechanisms. At the current state of research, these coefficients only affect the DL3 and DL4 displacement capacity; their values vary from 0.4 to 0.9 and were defined on expert judgement, benefitting from the evidence of empirical fragility curves. They are applied when structural details, such as tie rods or r.c. ring beams, are absent, with values that as a function of both the masonry quality (more punitive in case of irregular masonry) and the floor types (more punitive in case of vaults or very flexible floors). Moreover, drift thresholds for defining DL3 and DL4 were updated and differentiated according to the masonry type to be consistent with the up-to-date experimental evidence ([28], [29], [31]) and the EMS98 damage levels (see Table 5).

As for the evaluation of IM_{DL} , a corrective factor was introduced to IM_{DL} in order to account for the approximation that nonlinear static procedures imply with respect to more refined methods, as nonlinear dynamic analyses. In particular, on basis of the work done by Marino et al. [41] a corrective factor equal to 1.45 was applied. The values of ξ_{DL} were computed according to Cattari and Lagomarsino [42] varying the structural details of the schools. Moreover, the ADSR spectral shape was refined including, in the branch usually adopted at constant velocity, the dependence on an α coefficient (ranging from 1.1 to 1.4) to make it more consistent with evidence from actual recordings (see also [43]).

	Drift limit values for the shear (S) and flexural (F) response panels			
	S – DL3	S – DL4	F – DL3	F – DL4
Min	0.0025	0.0045	0.0035	0.007
Max	0.006	0.011	0.009	0.018

Table 5. Range of variation of drift thresholds adopted in *DBV-masonry* model.

4 COMPARISON OF RESULTS

The results obtained from the two analytical-mechanical methods are compared as follows, in terms of both intermediate calculation ratios and parameters describing the fragility curves (IM_{DLi} and β_{DLi}).

As for the first type of comparison, Figure 6 compares the parameter i_1 from the *Vulnus* approach, to for the value of the base shear capacity normalized to the total mass from the *DBV-Masonry* model.

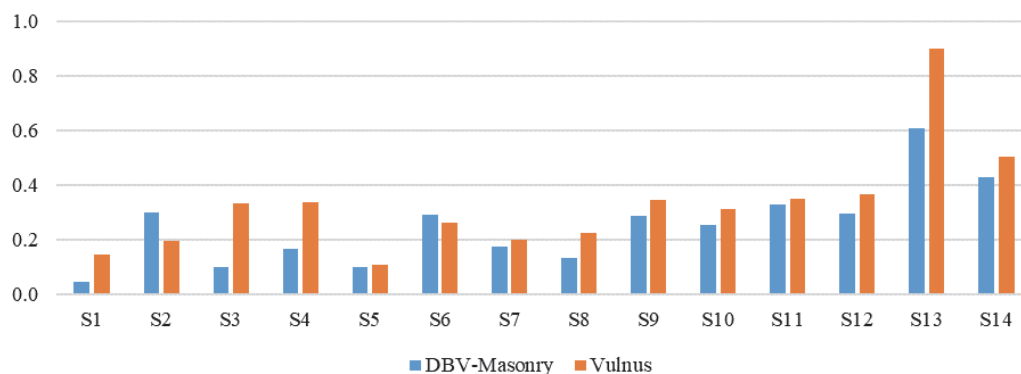


Figure 6. Comparison in terms of base shear normalized to total mass.

In general, a good correspondence is observed for most of schools. The highest difference, depicted in the cases S1, S3 and S4, is due to the strong penalization in the overall base shear capacity in the *DBV-Masonry* model given by the coefficients K_1 , K_2 , K_3 and K_4 , accounting

for poor structural details (e.g., the absence of tie rods and r.c. ring beams) and geometric irregularities. The complete set of corrective coefficients assigned to each school and applied to the overall base shear capacity are shown in Table 6. In the *Vulnus* procedure, in case of irregular buildings, the resistance area of walls is divided by a corrective factor (equal to 1.1) to consider the effects of the uneven distribution of stresses on the shear strength.

Ki factors of DVB- Masonry model	ID School													
	S1	S2	S3	S4	S5	S6	S7	S8	S9	S10	S11	S12	S13	S14
K₁	0.9	1.2	0.8	0.9	1.1	1.2	1.1	0.9	1	1.2	1.2	1.2	1.2	0.9
K₂	0.85	0.9	0.85	0.9	0.83	0.85	0.9	0.9	0.81	0.85	0.85	0.85	0.85	0.85
K₃	0.75	0.75	0.75	0.75	0.8	0.85	0.9	0.75	0.99	0.75	0.9	0.85	0.75	0.75
K₄	0.65	1	0.55	0.65	1	1	1	0.8	0.95	1	1	1	1	0.65

Table 6. Corrective factors used by DBV-Masonry model and applied to base shear capacity.

Figure 7 shows instead the comparison in terms of IM_{DLi} values. As recalled in §3.1, in the case of *Vulnus* approach, the value reported corresponds to a medium-severe damage level (DL2-3), whereas, in the case of the *DBV-Masonry* model, both values corresponding to DL2 and DL3 are reported separately. The comparison shows that in most cases the two models provide a good correspondence (such as for schools S1, S3, S4, S5, S9, S11 and S12), while in other cases the *DBV-Masonry* model provides greater median (less vulnerable structures) with respect to the *Vulnus* approach. This difference stems from the more significant role of the out-of-plane mechanisms, which are differently treated by the compared methods.

The values of the three indexes defined by the *Vulnus* approach are reported in Table 7; for schools with lower indexes i_2 , also with respect to their i_1 index, (i.e., structures more susceptible to OOP mechanisms) greater differences in the resulting IM_{DLi} values are found.

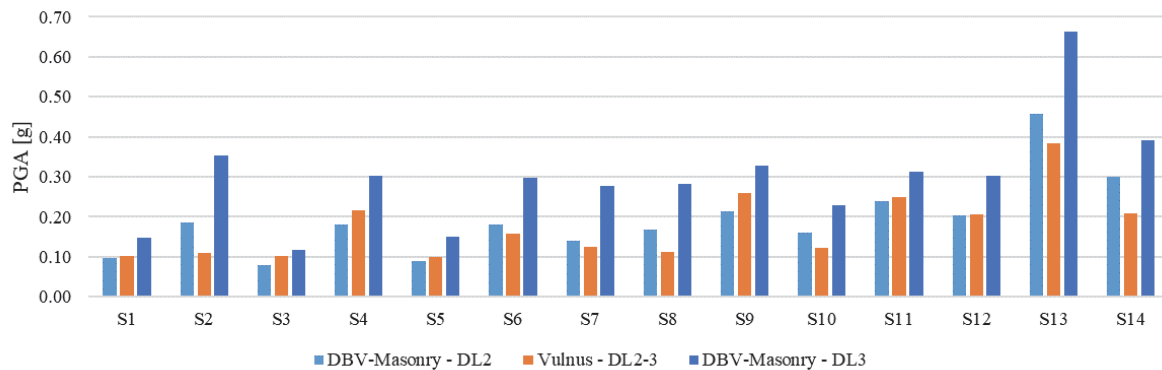


Figure 7. Comparison for the prototype schools in terms of median IM_{DLi} value (i.e., PGA in [g]).

Indexes Vulnus	Schools													
	S1	S2	S3	S4	S5	S6	S7	S8	S9	S10	S11	S12	S13	S14
i1 [a/g]	0.15	0.31	0.33	0.34	0.11	0.26	0.20	0.23	0.35	0.20	0.35	0.37	0.90	0.50
i2 [a/g]	0.16	0.10	0.09	0.27	0.14	0.18	0.15	0.12	0.31	0.11	0.30	0.20	0.36	0.19
i3	0.67	0.03	0.69	0.24	0.58	0.41	0.31	0.68	0.18	0.32	0.27	0.16	0.40	0.58

Table 7. Indexes obtained from *Vulnus* approach.

Indeed, in the *Vulnus* approach, the vulnerability of these schools is dominated by the activation of local mechanisms. Conversely, as described in §3.2, the *DBV-Masonry* model

includes the vulnerability associated to out-of-plane mechanisms only in a conventional way, by limiting the available global ductility.

Lastly, Figure 8 compares resulting fragility curves for some schools. As expected from the results illustrated in Figure 6 and Figure 7, for schools S9 and S11 the match of fragility curves is very good, while for schools S6 and S10 fragility curves derived from *Vulnus* approach are backward (describing a more vulnerable structure). This result is again mainly due to the different ways through which the two approaches treat the OOP mechanisms.

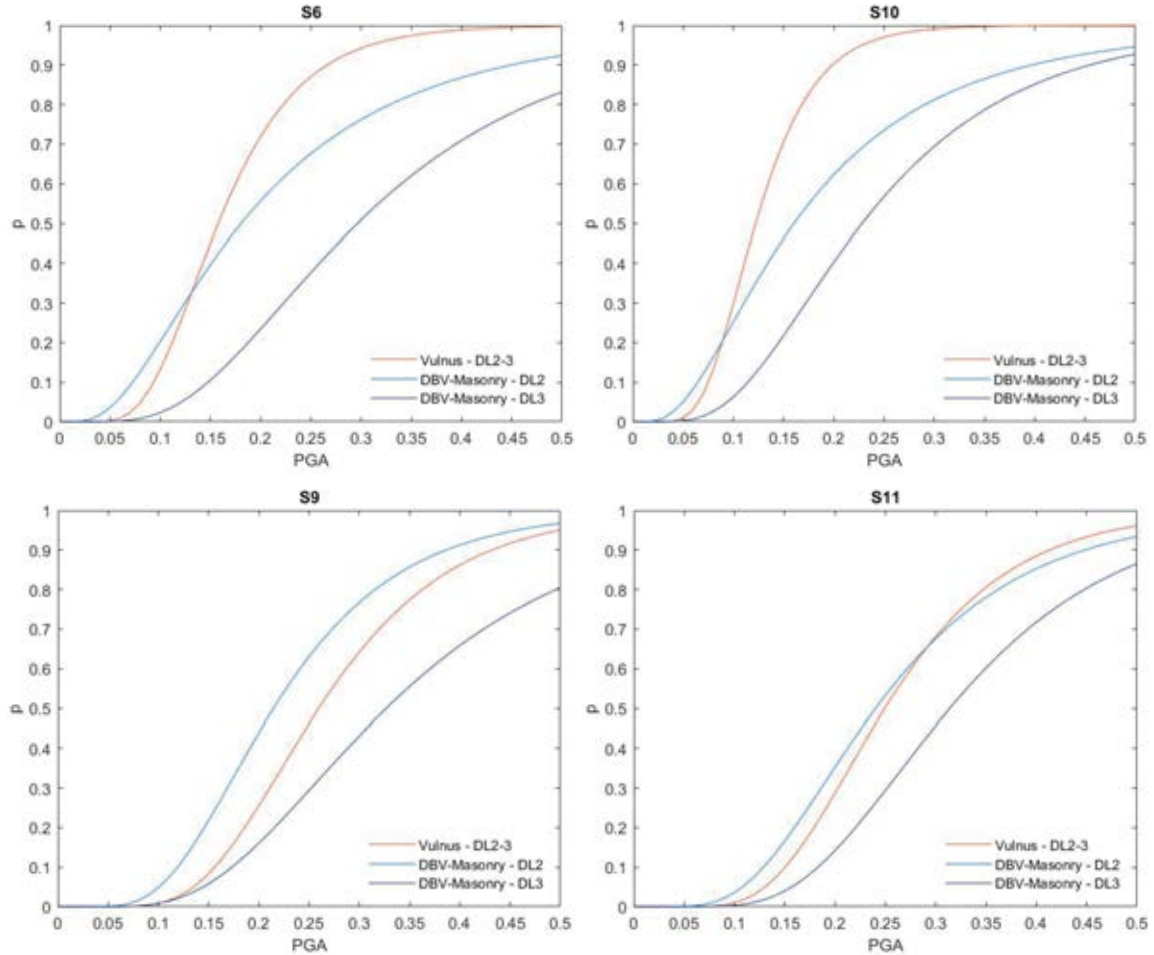


Figure 8. Comparison of fragility curves defined by DBV-Masonry (DL2 and DL3) and *Vulnus* approaches (DL2-3).

5 COMPARISON BETWEEN OBSERVED DAMAGE AND DPM ESTIMATED FROM FRAGILITY CURVES

As introduced in §2, some prototype schools were selected from those damaged and declared unusable after the seismic sequence that hit Central Italy in 2016/2017 [21]. Information on the actual damage of these schools was thereby available. These data are really valuable to preliminarily assess the reliability of the damage level estimated by fragility curves. Of course, a number of approximations were made to provide this comparison, since the aim of this study is far from an accurate simulation of the seismic response of these schools (e.g., made in other studies through refined 3D models and by performing nonlinear dynamic analyses [44]). Nevertheless, the comparison is useful in order to verify whether the damage predicted by fragility curves has the same order of magnitude of the observed damage; in addition, possible discrepancies might

emerge in the estimation of the consequences/losses when the fragility curves are then used for risk analyses scopes (e.g., [45]).



Figure 9. View of damaged schools S5, S9, and S11.

In order to make such a comparison, for each school an estimate is provided (Table 8) of the level of global damage observed and of the Peak Ground Acceleration that affected the structure ($PGA_{2016/2017}$). The damage level was derived as part of the survey activities described in Di Ludovico et al. [24], based on a homogeneous approach which is consistent with the damage levels defined by the EMS98 scale [20]. The estimate of $PGA_{2016/2017}$ is affected by more significant uncertainties. Only in one case (S9), the school, now demolished, was permanently monitored by the Italian Seismic Observatory of the Department of Civil Protection [46]. Thus, recorded data of the events that hit the school are available; in particular, the $PGA_{2016/2017}$ associated to the most intense recorded seismic event (October 26th, 2016) is equal to 0.47g.

Conversely, in other cases, the maximum $PGA_{2016/2017}$ value was derived from shake maps provided by INGV (Istituto Nazionale di Geofisica e Vulcanologia, INGV, <http://shake-map.rm.ingv.it/shake/index.html>). Attenuation laws and possible phenomena of amplification due to topography and stratigraphy, were considered, as well as third level seismic micro-zonation studies (MZ3), where available.

Specifically, for school S11, the PGA of the most significant event (August 24th, 2016) was defined equal to 0.30g, according to the shake maps provided by INGV. It was then multiplied by a coefficient equal to 1.2, in order to consider topographic amplification, consistently with Italian Code [47].

Concerning school S5, the PGA of the most severe event (October 26th, 2016) was derived from shake maps, equal to 0.15g. This school was subjected to strong phenomena of site effects, as confirmed by. Thus, a $PGA_{2016/2017}$ equal to 0.23g was estimated. Further detailed numerical studies confirmed that the combination of structural vulnerability and amplification phenomena played a fundamental role in the response of this school [48].

ID School	Observed DL	Stratigraphic amplification	Topographic amplification	Estimated $PGA_{2016/2017}$ for computing the DPM from fragility curves [g]		
				Event	PGA from shake maps	Adopted PGA
S5	4	FA=1.45-1.63 Soil B	Plain	26/10/2016	0.15	0.23
S9	4	FA=1.37 Soil B	Slight slope	26/10/2016	0.47 (recorded)	0.47 (recorded)
S11	3	Soil B	Ridge	24/08/2016	0.30	0.36

Table 8. Estimated damage level and PGA for damaged prototype schools

The estimated $PGA_{2016/2017}$ values were used to enter the fragility curves developed in §4 and then calculate the relative Damage Probability Matrix (DPM), and then the average damage level (μ_d) through the following expression:

$$\mu_D = \sum_{k=0}^5 p_k \cdot k \quad (1)$$

where p_k is the probability of reaching each damage grade k (from 1 to 5). As introduced in §3.2, the analytic-mechanical *DBV-Masonry* model allows fragility curves to be directly derived only for the first four damage levels. For the sake of comparisons, DL5 fragility curve was defined adopting a distance from DL4 curve consistent with the macroseismic model proposed by Lagomarsino and Giovinazzi [38] and adopted as reference also in the *Vulnus* model.

Figure 10 illustrates, for each school examined in this section, the fragility curves and the relative DPM; the vertical line in the graphs corresponds to the value of the $PGA_{2016/2017}$ reported in Table 8.

In order to compare the average damage level (μ_d) with the observed damage, the continuous variable μ_d shall be converted in a discrete number. To this aim, the binomial distribution was adopted [38], assuming that the upper bounds of each interval correspond to a probability of 0.5 in the associated cumulative distribution function. That leads to the conversion rule summarized in Table 9. The final values of the comparison are summarized in Table 10.

DLi	Conversion rule
1	$0.7 < \mu_d \leq 1.6$
2	$1.6 < \mu_d \leq 2.5$
3	$2.5 < \mu_d \leq 3.4$
4	$3.4 < \mu_d \leq 4.3$
5	$4.3 < \mu_d \leq 5$

Table 9. Criterion to convert the mean damage level into DLi discrete values.

Schools	Level of observed damage from real damage	Average damage level derived from fragility curves			
		Vulnus		DBV-Masonry	
		μ_D	DL	μ_D	DL
S5	4	3.67	4	3.21	3
S9	4	3.30	3	3.13	3
S11	3	2.87	3	2.78	3

Table 10. Comparison between observed and estimated damage levels from derived fragility curves.

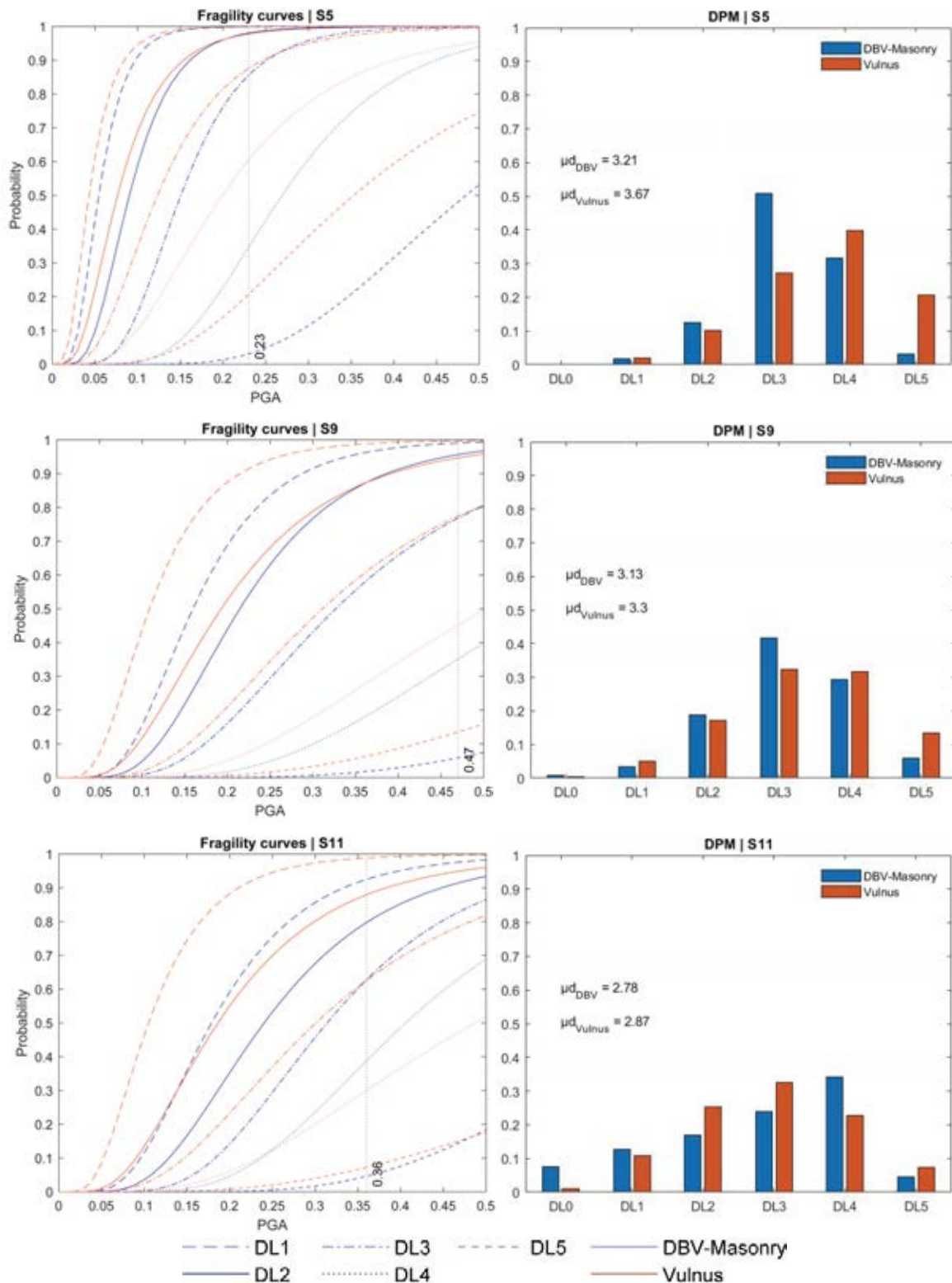


Figure 10. Comparison of fragility curves and DPM of damage prototype school buildings.

The comparison of results is satisfactory, in line with the general good correspondence discussed in §4.

In the case of school S5, the *DBV-Masonry* model slightly underestimates the damage level. In that case, the actual damage testified a clear dominance of the in-plane response of walls

(with very severe diagonal cracks in most piers of the first level, as shown in Figure 9) but also the activation of the out-of-plane response of part of the main façade. Thus, the aforementioned slight underestimation could be associated to the conventional way through which the *DBV-Masonry* model includes OOP mechanisms.

Concerning school S9, the results of both analytical-mechanical approaches slightly underestimate the actual damage level (i.e., the value of μ_D is close to the lower threshold value for DL4); however, it is worth highlighting that the school suffered from damage accumulation phenomena [44], neglected by the derived fragility curves. In fact, although the $PGA_{2016/2017}$ was associated to the most severe event, indeed some moderate damage already occurred due to the first shock (August 24th, 2016).

6 CONCLUSIONS

This paper has reported the comparison of results obtained from the application of two mechanical-analytical vulnerability models to a sample of 14 prototype schools, representative of the Italian school asset. In particular, the hybrid model based on the integrated use of mechanical and heuristic approach *Vulnus Vb 4.0-2009*, developed by the University of Padova, and the mechanical model *DBV-Masonry* developed by the University of Genoa were used. These vulnerability models aim at providing seismic vulnerability assessments of masonry buildings at territorial scale, to support seismic risk evaluations.

In this contribution, these approaches were applied to the selected prototype schools in their "as it is" configuration, to facilitate the comparison and without introducing the assumptions made necessary by the propagation of prototype buildings for the scopes of large scale assessment (as those addressed in MARS project illustrated in [17]).

The examined methods were compared in terms of derived fragility curves, as well as by analyzing intermediate parameters, such as the value of the base shear normalized to the total mass.

Results highlighted a good match between the two methods. The most relevant differences were found for buildings of which seismic vulnerability is potentially dominated by the trigger of local mechanisms; in these cases, the *DBV-Masonry* model, which takes into account the activation of out-of-plane mechanisms only conventionally, estimated a lower damage of the structure.

Lastly, the comparison between DPM estimated from fragility curves and observed damage has been provided for three schools of the sample, hit by the Central Italy earthquake. Results are promising and show a good capability of methods in forecasting the expected damage.

ACKNOWLEDGEMENTS

The results presented in the paper were achieved in the national research project ReLUIS-DPC 2019 -2021 (www.reluis.it), supported by the Italian Civil Protection Department and, in particular, in the Work Package 4 (WP4 – “Seismic Risk Maps -MARS”, Coord. Proff. S. Lagomarsino and A.Masi). Moreover, the Authors thank the members of research units of UniNA (University of Naples Federico II - Coord. Prof. M.Di Ludovico) and UniTS (University of Trieste, Coord. Prof. N.Gattesco) for the data provided regarding prototype schools examined in the paper.

REFERENCES

- [1] M. Di Ludovico, A. Digrisolo, C. Moroni, F. Graziotti, V. Manfredi, A. Prota, M. Dolce & G. Manfredi, Remarks on damage and response of school buildings after the Central Italy earthquake sequence. *Bull Earthquake Eng* **17**, 5679–5700, 2019. <https://doi.org/10.1007/s10518-018-0332-x>
- [2] M. Di Ludovico, A. Santoro, G. De Martino, C. Moroni, A. Prota, M. Dolce and G. Manfredi, Cumulative damage to school buildings following the 2016 central Italy earthquake sequence. *Bollettino di Geofisica Teorica ed Applicata* Vol. 60, n. 2, pp. 165-182, June 2019. DOI 10.4430/bgta0240
- [3] D. Gautam, R. Adhikari, R. Rupakhety and P. Koirala, An empirical method for seismic vulnerability assessment of Nepali school buildings. *Bull Earthquake Eng* **18**, 5965–5982, 2020. <https://doi.org/10.1007/s10518-020-00922-z>
- [4] H. Azizi-Bondarabadi, N. Mendes, P.B. Lourenço & N.H. Sadeghi, Empirical seismic vulnerability analysis for masonry buildings based on school buildings survey in Iran. *Bull Earthquake Eng* **14**, 3195–3229, 2016. <https://doi.org/10.1007/s10518-016-9944-1>
- [5] C. González, M. Niño & M.A. Jaimes, Event-based assessment of seismic resilience in Mexican school buildings. *Bull Earthquake Eng* **18**, 6313–6336, 2020. <https://doi.org/10.1007/s10518-020-00938-5>
- [6] D. D'Ayala, C. Galasso, A. Nassirpour, R.K. Adhikari, L. Yamin, R. Fernandez, D. Lo, L. Garciano and A. Oreta, Resilient communities through safer schools. *International Journal of Disaster Risk Reduction* Vol. 45, 2020. <https://doi.org/10.1016/j.ijdrr.2019.101446>
- [7] UNISDR, Comprehensive School Safety, United Nations Office for Disaster Risk Reduction (UNDRR), 2014
- [8] WISS, Worldwide Initiative for Safe Schools - Vision: by 2030, Every School Will Be Safe, United Nations Office for Disaster Risk Reduction (UNDRR), 2013
- [9] A. Muñoz, M. Blondet, R. Aguilar, M. A. Astorga. Empirical fragility curves for Peruvian school buildings. *ERES 2007*. DOI 10.2495/ERES070261
- [10] N. Giordano, F. De Luca, A. Sextos, F. Ramirez Cortes, C. Fonseca Ferreira & J. Wu, Empirical seismic fragility models for Nepalese school buildings. *Natural Hazards*, 2020. <https://doi.org/10.1007/s11069-020-04312-1>
- [11] M. Yekrangnia, A. Bakhshi, M.A. Ghannad & M. Panahi, Risk assessment of confined unreinforced masonry buildings based on FEMA P-58 methodology: a case study—school buildings in Tehran. *Bull Earthquake Eng* **19**, 1079–1120, 2021. <https://doi.org/10.1007/s10518-020-00990-1>
- [12] N. Giordano, F. De Luca & A. Sextos, Analytical fragility curves for masonry school building portfolios in Nepal. *Bull Earthquake Eng* **19**, 1121–1150, 2021. <https://doi.org/10.1007/s10518-020-00989-8>
- [13] C. Michel, P. Hannewald, P. Lestuzzi, D. Fäh & S. Husen, Probabilistic mechanics-based loss scenarios for school buildings in Basel (Switzerland). *Bull Earthquake Eng* **15**, 1471–1496, 2017. <https://doi.org/10.1007/s10518-016-0025-2>

- [14] P. Hannewald, C. Michel, P. Lestuzzi, H. Crowley, J. Pinguet & D. Fäh, Development and validation of simplified mechanics-based capacity curves for scenario-based risk assessment of school buildings in Basel. *Engineering Structures* Vol 209, 2020. <https://doi.org/10.1016/j.engstruct.2020.110290>
- [15] Italian Civil Protection Department (2018) National Risk Assessment 2018. Overview of the potential major disasters in Italy. Updated December 2018
- [16] M. Dolce, A. Prota, B. Borzi, F. da Porto, S. Lagomarsino, G. Magenes, C. Moroni, A. Penna, M. Polese, E. Speranza, G.M. Verderame, G. Zuccaro, Seismic risk assessment of residential buildings in Italy. *Bull Earthquake Eng* , 2020. <https://doi.org/10.1007/s10518-020-01009-5>
- [17] A. Masi, S. Lagomarsino, M. Dolce, V. Manfredi & D. Ottonelli, Towards the updated Italian seismic risk assessment: exposure and vulnerability modelling. *Bull Earthquake Eng*, 2021. <https://doi.org/10.1007/s10518-021-01065-5>
- [18] M. Donà, P. Carpanese, V. Follador, L. Sbrogio, F. da Porto, Mechanics-based fragility curves for Italian residential URM buildings, *Bull Earthquake Eng* ,1–34, 2020. <https://doi.org/10.1007/s10518-020-00928-7>
- [19] S. Lagomarsino, S. Cattari, Fragility Functions of Masonry Buildings, in K. Pitilakis et al. (eds.), SYNER-G: Typology Definition and Fragility Functions for Physical Elements at Seismic Risk, Geotechnical, Geological and Earthquake Engineering 27, 2014. DOI 10.1007/978-94-007-7872-6_5.
- [20] G. Grunthal, EMS98 - European Macroseismic Scale 1998, Conseil de l'Europe - Cahiers du Centre Européen de Géodynamique et de Séismologie, Luxembourg, 1998.
- [21] D. Ottonelli, S. Alfano, S. Cattari, M. Di Ludovico and A. Prota, Analisi statistiche dei dati tipologici e di danno delle scuole in muratura danneggiate dal terremoto del Centro Italia 2016/2017. *XVIII Convegno ANIDIS, L'ingegneria Sismica in Italia*. Settembre 15-19, Ascoli Piceno, Italia, 2019. (in Italian)
- [22] E. Saler, P. Carpanese, V. Pernechele and F. da Porto, Priority-ranking procedure to assess seismic vulnerability of school buildings at territorial scale. *XVIII Convegno ANIDIS, L'ingegneria Sismica in Italia*. Settembre 15-19, Ascoli Piceno, Italia, 2019.
- [23] N. Gattesco, I. Boem, Classificazione degli edifici scolastici in muratura in Friuli-Venezia Giulia, finalizzata alla costruzione di modelli di rischio. *XVIII Convegno ANIDIS, L'ingegneria Sismica in Italia*. Settembre 15-19, Ascoli Piceno, Italia, 2019. (in Italian)
- [24] M. Di Ludovico, C. Moroni, D. Abruzzese, A. Borri, B. Calderoni, S. Caprili, A. Dall'Asta, F. da Porto, G. De Martino, G. de Matteis, B. Ferracuti, S. Lagomarsino, G. Magenes, A. Mannella, A. Marini, A. Masi, C. Mazzotti, C. Nuti, A. Santoro, L. Sorrentino, E. Spacone, G.M. Verderame, A. Prota, M. Dolce, G. Manfredi, Il contributo di ReLUIIS nelle attività di supporto all'emergenza sismica del Centro Italia 2016. *XVIII Convegno ANIDIS, L'ingegneria Sismica in Italia*. Settembre 18-21, Pistoia, Italia, 2017. (in Italian)
- [25] E. Saler, V. Follador, P. Carpanese, F. da Porto, Fragility assessment of the Italian masonry school building asset for risk evaluation at national scale. *COMPDYN*, 28–30 June 2021, Streamed from Athens, Greece, 2021.

- [26] N. Augenti, F. Parisi, E. Acconcia, MADA: online experimental database for mechanical modelling of existing masonry assemblages *Proc. of the 15th World Conference on Earthquake Engineering*, Lisbon, 2012.
- [27] M. Krzan, S. Gostic, S. Cattari and V. Bosiljkov, Acquiring reference parameters of masonry for the structural performance analysis of historical building, *Bull. Earth. Eng.*, 13(1), 203-236, 2015.
- [28] F. Vanin, D. Zaganelli, A. Penna and K. Beyer, Estimates for the stiffness, strength and drift capacity of stone masonry walls based on 123 quasi-static cyclic tests reported in the literature. *Bull. Earth. Eng.*, 15(12), 2017, 5435-5479
- [29] P. Morandi, L. Albanesi, F. Graziotti, T. Li Piani, A. Penna and G. Magenes, Development of a dataset on the in-plane experimental response of URM piers with brick and blocks, *Construction and Building Materials*, 190, 593-611, 2018.
- [30] S. Boschi, L. Galano and A. Vignoli, Mechanical characterization of Tuscany masonry typologies by in situ tests, *Bull Earthquake Eng.*, 17(1), 413-438, 2019.
- [31] A. Rezaie, M. Godio and K. Beyer, Experimental investigation of strength, stiffness and drift capacity of rubble stone masonry walls, *Construction and Building Materials*, 251, 118972, 2020.
- [32] MIT 2019, Ministry of Infrastructures and Transportation, Circ. C.S.LI.PP. No. 7 of 21/1/2019. Istruzioni per l'applicazione dell'aggiornamento delle norme tecniche per le costruzioni di cui al Decreto Ministeriale 17 Gennaio 2018. G.U. S.O. n.35 of 11/2/2019. (In Italian)
- [33] A. Borri, M. Corradi, G. Castori, A. De Maria, A method for the analysis and classification of historic masonry, *Bull Earthquake Eng.*, 13(9), 2647-2665, 2015.
- [34] M. Vettore, M. Donà, P. Carpanese, V. Follador, F. da Porto and M.R. Valluzzi, A Multilevel Procedure at Urban Scale to Assess the Vulnerability and the Exposure of Residential Masonry Buildings: The Case Study of Pordenone, Northeast Italy, *Heritage*. 3 1433–1468, 2020. <https://doi.org/10.3390/heritage3040080>.
- [35] A. Bernardini, R. Gori, C. Modena, M.R. Valluzzi, *Vulnus 4.0 - Automatic procedure for the seismic vulnerability analysis of masonry buildings*, 2009. (in Italian)
- [36] M.R. Valluzzi, User Manual of *Vulnus 4.0*, original program by Bernardini Gori A, Modena R C, Vb version edited by Valluzzi MR, with contributions by Benincà G, Barbetta E, Munari M, 2009. (in Italian)
- [37] GNDT-SSN, Scheda di esposizione e vulnerabilità e di rilevamento danni di primo livello e secondo livello (muratura e cemento armato), (1994). (in Italian)
- [38] S. Lagomarsino, S. Giovinazzi, Macroseismic and mechanical models for the vulnerability and damage assessment of current buildings, *Bull Earthquake Eng.* 4 415–443, 2006. <https://doi.org/10.1007/s10518-006-9024-z>.
- [39] S.A. Freeman, The capacity spectrum method as a tool for seismic design. In: *Proceedings of 11th European conference of earthquake engineering*, Paris, France, 1998.
- [40] L.C. Pagnini, R.S. Vicente, S. Lagomarsino, H. Varum H, A mechanical model for the seismic vulnerability assessment of old masonry buildings. *Earthquake and Structures* 2(1):25–42, 2011.

- [41] S. Marino, S. Cattari, S. Lagomarsino, Are the nonlinear static procedures feasible for the seismic assessment of irregular masonry buildings? *Engineering Structures*, 200, 109700, 2019.
- [42] S. Cattari and S. Lagomarsino, “Masonry structures,” 151–200. in T. Sullivan and G. M. Calvi (ed.) *Developments in the Field of Displacement Based Seismic Assessment*. IUSS Press and EUCENTRE, Pavia, Italy, p 524, ISBN, 978-88-6198-090-7, 2013.
- [43] C. Smerzini, C. Galasso, I. Iervolino, R. Paolucci, Ground motion record selection based on broadband spectral compatibility, *Earthquake Spectra*, 30(4):1427-1448, 2014.
- [44] A. Brunelli, F. de Silva, A. Piro, F. Parisi, S. Sica, F. Silvestri and S. Cattari, Numerical simulation of the seismic response and soil–structure interaction for a monitored masonry school building damaged by the 2016 Central Italy earthquake. *Bull Earthquake Eng* . 19, 1181–1211, 2021. <https://doi.org/10.1007/s10518-020-00980-3>
- [45] A.W. Coburn, R.J.S. Spence, *Earthquake protection*, 2nd edn. Wiley, 2002.
- [46] S. Cattari, S. Degli Abbati, D. Ottonelli, C. Marano, G. Camata et al, Discussion on data recorded by the Italian structural seismic monitoring network on three masonry structures hit by the 2016–2017 Central Italy earthquake. *COMPDYN*, 24–26 June 2019, Crete, Greece, DOI 10.7712/120119.7044.20004.
- [47] NTC (2018) *Norme Tecniche per le Costruzioni*. DM 17/1/2018, Italian Ministry of Infrastructure and Transportation, G.U. n. 42, 20 February 2018, Rome, Italy (in Italian)
- [48] S. Cattari, S. Alfano, A. Brunelli, M. Angiolilli & F. De Silva, Investigating the combined role of the structural vulnerability and site effects on the seismic response of a URM school hit by the central Italy 2016 earthquake, 2021. *Submitted to Structures*.